Advances in Applied Energy 9 (2023) 100115

Contents lists available at ScienceDirect

Advances in Applied Energy

journal homepage: www.elsevier.com/locate/adapen

A distributed robust control strategy for electric vehicles to enhance resilience in urban energy systems

Zihang Dong [a], Xi Zhang [b,c,*], Ning Zhang [d], Chongqing Kang [d], Goran Strbac [a]

[a] Department of Electrical and Electronic Engineering, Imperial College London, London, SW7 2AZ, U.K.
[b] Department of Grid Digitalization Technology, State Grid Smart Grid Research Institute Co., Ltd, Beijing, 102209, China
[c] State Grid Laboratory of Electric Power Communication Network Technology, Nanjing, Jiangsu, 210003, China
[d] State Key Laboratory of Power System, Department of Electrical Engineering, Tsinghua University, Beijing, 100084, China

ARTICLE INFO

Keywords:
Multi-energy micro-grid system
Electric vehicle
Power system resilience
Distributed control strategy

ABSTRACT

Resilient operation of multi-energy microgrid is a critical concept for decarbonization in modern power system. Its goal is to mitigate the low probability and high damaging impacts of electricity interruptions. Electrical vehicles, as a key flexibility provider, can react to unserved demand and autonomously schedule their operation in order to provide resilience. This paper presents a distributed control strategy for a population of electrical vehicles to enhance resilience of an urban energy system experiencing extreme contingency. Specifically, an iterative algorithm is developed to coordinate the charging/discharging schedules of heterogeneous electrical vehicles aiming at reducing the essential load shedding while considering the local constraints and multi-energy microgrid interconnection capacities. Additionally, the gap between electrical vehicle energy and the required energy level at the departure time is also minimised. The effectiveness of the introduced distributed coordinated approach on energy arbitrage and congestion management is tested and demonstrated by a series of case studies.

1. Introduction

In recent years, the occurrence frequency of extreme natural disasters, e.g., earthquakes, hurricanes, floods and ice storms, has dramatically increased due to climate change, causing severe power outage. For instance, Hurricane Irene in 2011 and Superstorm Sandy in 2012 both caused massive power outages in Houston and Manhattan, respectively [1,2]. Seven of the ten major storms in the last four decades have happened in the last ten years, each of which has resulted in significant economic loss over 1 billion dollars [3]. Such incidents are uncommon and hence unanticipated, but their influence on power systems is enormous. All these pose threats to the social utility, even people's lives. Therefore, enhancing resilience, which is defined as"the ability to withstand and reduce the magnitude and/or duration of disruptive events, which includes the capability to anticipate, absorb, adapt to, and/or rapidly recover from such events" [4], has recently been recognised as the key driver of the energy community to reduce the possible damage caused by these catastrophes. When the transmission network breaks down due to extreme conditions, there may be a sudden gap between generation supply and power demand so that the main grid is facing challenges in maintaining the stability of the power system. Under this circumstance, the islanding of microgrid (MG) is a solution for more resilient power system and it can alleviate the supply burden of the main grid during emergencies. Thanks to the disconnection of MG, the main grid can reallocate spare resources to the grid-connected loads. Since the maintenance of load supply during contingencies is a key objective of resilient systems, resilience, as used in this paper, means the ability to reduce the load curtailment considering the criticality of loads during disruptive events, such as outage of utility power supply under the extreme weather condition. Given the significant disruptions caused by extreme events, a resilient electrical system should be focused on restoring essential loads (e.g. medical services and emergency lighting) [5].

The traditional method in the period of power outage is to shut down the failing plants, leaving the rest of the grid to cope as best as it can in order to satisfy the demand. Nowadays, MG is employed to provide practicable solutions to address the challenge of enhancing resiliency [6]. Compared to large power transmission network, MGs are less vulnerable to disaster events like hurricanes, blizzards etc., because of their ability of islanding and little geographical areas [7]. In particular, MGs can provide higher load reliability compared to bulk power systems [8]. The feasibility of MGs as a resiliency resource is analysed in [9]. If the utility power supply is completely or partially interrupted during extreme events, distributed generators in MGs, such as diesel generators, wind turbines, and photovoltaics, can restore local loads via islanding schemes or global critical loads via dynamic boundaries and formation.

* Corresponding author.
E-mail address: zhangxi1@geiri.sgcc.com.cn (X. Zhang).

https://doi.org/10.1016/j.adapen.2022.100115
Received 26 September 2022; Received in revised form 1 December 2022; Accepted 3 December 2022
Available online 7 December 2022

Indices and sets

$t \in \mathcal{T}$	Index and set of time instants
$m \in \mathcal{M}$	Index and set of microgrid
$j \in \mathcal{N}$	Index and set of EVs
$n \in \mathcal{L}$	Index and set of transmission lines
$\mathcal{N}_m \subseteq \mathcal{N}$	The set of EVs at microgrid m
$\mathcal{A}_j \subseteq \mathcal{T}$	Available time window of EV j
$\mathcal{P}_j^{EV}$	Set of feasible operational profiles of EV j

Parameters

Δt	Time discretization step [h]
$\overline{P}_m^{\mathrm{UG}}$	Maximum utility supply to microgrid m [MW]
$\overline{P}_m^{\mathrm{CG}}$	Maximum controllable power at microgrid m [MW]
$\overline{C}_l^{\mathrm{L}}$	Capacity of transmission line l [MW]
$\overline{P}_j^{\mathrm{EV}}$	Maximum charging rate of EV j [MW]
$\underline{P}_j^{\mathrm{EV}}$	Maximum discharging rate of EV j [MW]
t_j^{in}	Plug-in time of EV j [h]
t_j^{out}	Plug-out time of EV j [h]
η_j	Battery charging efficiency of EV j [p.u.]
$\overline{SOC}_j$	Maximum state of charge of EV j [p.u.]
$\underline{SOC}_j$	Minimum state of charge of EV j [p.u.]
SOC_j^r	Required SOC of EV j [p.u.]
E_j^r	Total required energy of EV j [MWh]
$\bar{E}_j$	Maximum battery capacity of EV j [MWh]
$D_{m,t}^{\mathrm{EL}}$	Essential demand of microgrid m at time t [MW]
$D_{m,t}^{\mathrm{NEL}}$	Non-essential demand of microgrid m at time t [MW]
$\overline{P}_{m,t}^{\mathrm{RE}}$	Maximum RES power of microgrid m at time t [MW]
$c_{m,t}^{\mathrm{UG}}$	Electricity price of the utility grid [£/MWh]
$c_{m,t}^{\mathrm{CG}}$	Electricity price of the controllable generation power [£/MWh]
I_t^{HILP}	Binary indicator of the microgrid operation mode [p.u.]
α_m^{RE}	RES curtailment coefficients [p.u.]
$\alpha_m^{\mathrm{EL}}, \beta_m^{\mathrm{EL}}$	Essential load curtailment coefficients [p.u.]
$\alpha_m^{\mathrm{NEL}}, \beta_m^{\mathrm{NEL}}$	Non-essential load curtailment coefficients [£/MW]

Variables

$P_{j,t}^{\mathrm{EV}}$	Electricity power of EV j at time t [MW]
$SOC_{j,t}$	State of charge of EV j at time t [p.u.]
$D_{m,t}$	Aggregate demand at microgrid m at time t [MW]
D_t	Aggregate demand at time t [MW]
$P_{m,t}^{\mathrm{UG}}$	Utility grid supply to microgrid m at time t [MW]
$P_{m,t}^{\mathrm{CG}}$	Controllable generation power at microgrid m at time t [MW]
$P_{m,t}^{\mathrm{RE}}$	RES power at microgrid m at time t [MW]
$C_{l,t}^{\mathrm{L}}$	Power flow at line l and time t [MW]
$Cur_{m,t}^{\mathrm{EL}}$	Essential load curtailment at microgrid m and time t [MW]
$Cur_{m,t}^{\mathrm{NEL}}$	Non-essential load curtailment at microgrid m and time t [MW]
$Cur_{m,t}^{\mathrm{EV}}$	Total EV load curtailment at microgrid m and time t [MW]
$\lambda_{m,t}^{NM}$	Marginal cost in normal mode [£/MWh]
$\lambda_{m,t}^{IM}$	Marginal cost in island mode [£/MWh]
$\lambda_{m,t}$	Marginal cost to coordinate the EV rescheduling [£/MWh]
$\bar{t}$	Power shifting in time instant [h]
$\underline{t}$	Power shifting out time instant [h]
$\underline{\delta}$	Maximum shifting power from $\underline{t}$ to $\bar{t}$ [MW]
$a(P^{EV}, j, \bar{t})$	Maximum feasible power increase of EV j at $\bar{t}$ [MW]
$b(P^{EV}, j, \underline{t})$	Maximum feasible power decrease of EV j at $\underline{t}$ [MW]
$c(P^{EV}, j, \underline{t}, \bar{t})$	Maximum power shift due to energy limit [MW]
$d(P^{EV}, j, \bar{t})$	Maximum power increase due to local capacity [MW]
$e(C^{\mathrm{L}}, P^{EV}, j, \bar{t}, \bar{t})$	Maximum power shift due to line capacity [MW]
RTM_j	Response time margin [h]
$SOCM_j$	State of charge margin [p.u.]
RMR_j	Response margin ratio [p.u./h]

Functions

C_{Total}	Total operational and penalty cost
$\tilde{C}_{m,t}^k$	Penalty function of load curtailment
f_m	Penalty function of RES curtailment

In addition to employing MGs as a resiliency resource, researchers have paid much attention on the planning and operational strategies utilised by MGs to enhance their resilience during significant outage events. Reference [10] presents an optimal planning model for smart multi-energy systems, with traffic flow guidance used to capture vehicle routing and charging/discharging patterns. An agent-based day-to-day dynamic model to analyze the resilience of the transport network suffering from different levels of disruptions is proposed in [11]. In [12], a two-stage optimisation model capturing both normal and emergency situations is proposed to solve the investment problem of MEMGs towards load restoration after natural disasters. A planning method to determine the optimal configuration of distribution level multi-energy system considering the comprehensive impacts from supply, network and demand sides is provided in [13]. Reference [14] presents a two-stage energy management technique based on hierarchical control to minimise the system operation cost and dispatching real-time energy in networked MGs with high renewable penetration. In [15], a spatial-temporal transportable energy storage system model is proposed to mitigate the customer interruption cost and power generation expense. The authors of [16] propose a refined and executable post-disaster restoration scheduling approach for cyber-physical power distribution systems considering the dynamic formation, expansion and integration of MGs.

Furthermore, much research has been performed on different aspects of the Vehicle to Grid (V2G) concept, such as, frequency and voltage regulation [17], renewable energy source integration [18], and energy arbitrage [19]. To enhance the system resilience, the deployment of electric vehicles (EVs) providing backup power under outage of the external electric grid has also been investigated. In [20], an optimisation model that aims at maximizing backup duration and an algorithm for energy resources scheduling are developed. Reference [21] investigates the feasibility of providing power to residential customers during power outages in order to improve a distribution system's resilience. Resilient routing and scheduling of mobile power sources are investigated via a two-stage framework in [22]. The optimal utilization of EVs parking at a shared station to enhance energy resilience for two residential and commercial buildings is presented in [23]. Reference [24] explores the impact of adaptive signal control within a doubly dynamic learning framework on the resilience of urban road networks. The authors of [25] conduct a research and analysis of the benchmarks for the immunity of multi-scale urban road networks against global disruptions.

While numerous EVs with heterogeneous parameters are involved in the MEMG system, it would be challenging to carry out an optimisation-based centralized control, especially with a nonlinear resilience-oriented objective function. In distributed control, as opposed to centralized control, each EV owner decides whether to charge or discharge the battery according to their specific purpose, which is usually to minimise the individual energy cost in normal operation mode and maximise system

benefit via V2G service during the grid outage period. Due to the lack of direct control in the distributed method, achieving the optimal global solution is not always guaranteed. Additionally, because the distributed control divides the computational burden between EVs, and each EV solves its own charge and discharge problem, the distributed method is highly scalable and suitable for large-scale EV fleets. To reduce the need for communication between EVs in the distributed control structure, an aggregator can be used to aggregate information and send to EVs control signals, which is usually price-based [26].

Classical distributed and decentralized optimisation algorithms based on Lagrangian relaxation such as dual decomposition [27] or alternating direction method of multipliers (ADMM) [28] are guaranteed to converge only for convex and separable problems. In [29], a partial decomposition method based on the Lagrangian relaxation framework is proposed for the distributed charging control of EVs considering the transmission grid congestion. Reference [30] introduces a hierarchical distributed method based on the exchange problem for the optimal charging coordination problem that is solved by ADMM. However, a drawback of the standard ADMM method is that the price signals based on global information cannot be updated accordingly after some participants change their operational schedules. In [31], a distributed hierarchical EV coordination mechanism is presented to exploit the synergies between the renewable distributed energy resources (DER) and EV charging needs. A decentralized charging strategy is presented in [32] to fill the valleys in a residential distribution network, and a shrunken-primal-dual subgradient algorithm is proposed to solve the problem in a decentralized manner. In [33], a distributed simulation-based policy improvement method developed from heuristic or experience-based policies demonstrates good performance and scalability. Reference [34] develops a consensus algorithm for distributed control of large-scale EV charging to reduce total charging power loss or provide V2G service with maximum available EV power. In [35], a decentralized charging control mechanism is proposed using historical three-phase voltage magnitude data from each EV charging point and there is no requirement of communication between controllers. In [36], a multi-agent deep reinforcement learning-based algorithm for the coordinated charging of EVs is proposed to reduce the energy cost while ensuring a high battery energy level before daily trips. Moreover, in [37], a practical demand response program for plug-in hybrid EVs charging scheduling based on the non-cooperative game theory framework is developed to optimise the EV charging cost. Although various distributed EV charging control algorithms have been investigated in the literature (see survey papers [38,39]), there is no existing method that is focusing on the coordination of bi-directional power flow between numerous heterogeneous EVs and the power system while simultaneously considering the transmission grid congestion, especially with the aim of reducing essential load curtailment in contingencies. In this context, a new distributed optimisation algorithm that can address these issues in the resilience problem is expected.

This paper proposes a novel multi-phase distributed control strategy which is, for the first time, used for numerous heterogeneous EVs to enhance resilient operation of MEMGs experiencing extreme events. The presented method mitigates the load curtailment iteratively by adjusting EV charging/discharging operations and minimises the gap between EV energy and the corresponding energy requirement at departure. Power exchange among multiple MEMGs are considered to achieve the optimal use of distributed energy resources. Consequently, the main contributions of this paper can be summarized as follows:

- A multi-phase distributed control strategy for EVs is proposed to enhance resilient operation of MEMGs. Driven by the price/penalty signal, every EV reschedules its charging/discharging profile temporally to provide V2G service minimising load curtailments during outage and the gap between EV energy and the corresponding requirement at departure.
- The interconnection capacity between MEMGs and the diversified distribution level constraints are simultaneously considered in the proposed algorithm. Therefore, EVs in different MEMG clusters can exchange energy based on spatial and temporal flexibility to reduce the overall load curtailment while preventing power networks from being overloaded.
- A smart load curtailment management approach is performed in case studies to ensure the imbalance of supply and demand does not experience major fluctuation so that the threats to the operation stability of the MEMG will be effectively mitigated.
- Compared to the traditional optimisation-based energy management methods, the proposed distributed algorithm effectively protects EV privacy while significantly reduces computational complexity. This is particularly advantageous when more MEMGs and numerous EVs are involved.

The rest of this paper is organized as follows. Section 2 introduces the model of flexible EVs and the electricity market. Subsequently, the proposed multi-phase distributed control strategy is described in Section 3. Numerical results based on a series of case studies aimed at evaluating the performance of proposed control strategy are demonstrated in Section 4, and Section 5 concludes this paper.

2. System model

2.1. The structure of MEMG cluster

Fig. 1 depicts the configuration of a MEMG cluster. Each MEMG can potentially comprise different components covering electricity, heat, gas and transport sectors. Particularly regarding distributed generation resources, PV and controllable generators (CGs), e.g., diesel generators and CHP, are considered to supplement the utility grid for local energy supply. MEMGs characterized by different functionalities e.g., commercial, industrial and residential, operate as independent complex during normal periods, and can be interconnected under extreme conditions such that the energy resources are shared and reallocated to collectively defend against disruptive events. In each MEMG, there are plug-in EVs that are expected to be charged. These EVs can increase flexibility to the system, but they will not provide services at the expense of losing energy in the battery, i.e., the energy level while they are connected to the grid cannot be lower than the initial energy level. The focus of this work is coordinating numerous V2G-capable EVs across MEMG cluster to mitigate load curtailment under extreme conditions, thereby enhancing the resilience of urban energy systems.

Let us denote the set of clustered MEMGs by $\mathcal{M} = \{1, \cdots, M\}$. For each MEMG, $m \in \mathcal{M}$, there are $\mathcal{N}_m = \{1, \cdots, N_m\}$ EVs participating in the resilience enhancement scheme. Thus, the total number of involved EVs is $N = \sum_{m\in\mathcal{M}} N_m$ and the corresponding set of EVs is denoted by $\mathcal{N} = \cup_{m\in\mathcal{M}}\mathcal{N}_m$. The analysis is performed over a discrete time interval $\mathcal{T} = \{1, \cdots, T\}$, with discretization step Δt.

2.2. Modelling of a single EV

The rated charging/discharging power of EV $j \in \mathcal{N}$ is denoted by $\overline{P}_j^{\mathrm{EV}} / \underline{P}_j^{\mathrm{EV}}$. EVs can only interact with MEMGs when connected to the chargers, so an availability window $\mathcal{A}_j \subseteq \mathcal{T}$ is assigned to EV j such that the power exchange with the grid $P_{j,t}^{\mathrm{EV}} = 0, \forall t \in \mathcal{T} \setminus \mathcal{A}_j$. Considering the uncertainties of EV driving plan, individual estimated arriving and departure time is given as a range, i.e., $[\tilde{t}_j^{in}, t_j^{in}]$ and $[t_j^{out}, \tilde{t}_j^{out}]$ respectively, as shown in Fig. 2. The most conservative EV availability window $\mathcal{A}_j = \{t_j^{in}, t_j^{in}+1, \cdots, t_j^{out}\}$ ranging from the latest arrival time t_j^{in} to the earliest departure time t_j^{out} based on individual estimation is used for EV dispatch to ensure the robustness of the EV dispatch strategy. Note that the optimality loss due to conservatism can be reduced by introducing rolling optimisation techniques with the latest estimation of EV driving plan. Let us denote the state of charge (SOC) of EV j at time

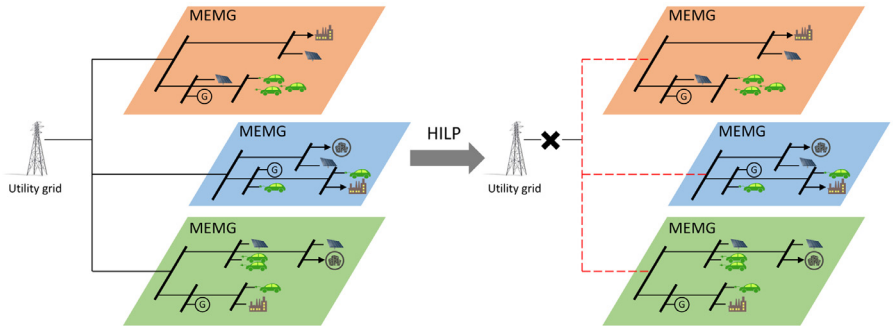

Fig. 1. The architecture of a MEMG cluster.

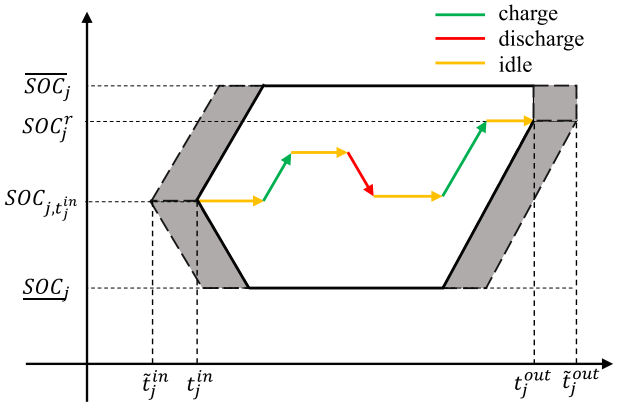

Fig. 2. Feasible SOC polygon of EV j and an example operational profile.

t by $SOC_{j,t}$, then the feasible set of power exchange profiles for EV j is represented by:

$$\begin{aligned}\mathcal{P}_j^{\mathrm{EV}} = \{P_j^{\mathrm{EV}} \in \mathbb{R}^T \mid \quad & \underline{P_j^{\mathrm{EV}}} \cdot \mathbb{1}_j(t) \le P_{j,t}^{\mathrm{EV}} \le \overline{P_j^{\mathrm{EV}}} \cdot \mathbb{1}_j(t), \\ & SOC_{j,t} = SOC_{j,t-1} + \eta_j \frac{P_{j,t}^{\mathrm{EV}}}{\bar{E}_j} \Delta t, \\ & \underline{SOC_j} \le SOC_{j,t} \le \overline{SOC_j},\ \forall t \in \mathcal{T}\}\end{aligned} \tag{1}$$

where η_j denotes the power exchange efficiency, $\bar{E}_j$ is the energy capacity of EV battery, and $\mathbb{1}_j$ is the indicator function:

$$\mathbb{1}_j(t) = \begin{cases} 1 & \text{if } t \in \mathcal{A}_j \\ 0 & \text{if } t \notin \mathcal{A}_j \end{cases} \tag{2}$$

The SOC of EV j is bounded by the maximum/minimum values $\overline{SOC_j}/\underline{SOC_j}$. For the specific scenario where EV j prioritises individual energy, this EV only agrees to provide flexibility and refuses to support other loads by losing its energy to be lower than the initial SOC at plug-in time. In this scenario, the lower limit $\underline{SOC_j}$ in (1) has to be replaced by $SOC_{j,t_j^{in}}$.

It is noted that every EV is required to be charged to an energy level SOC_j^r at the end of its availability window t_j^{out}. For an initial energy level $SOC_{j,t_j^{in}}$, the total energy exchange between EV and the grid should be no less than

$$E_j^r = \left(SOC_j^r - SOC_{j,t_j^{in}}\right) \cdot \bar{E}_j \tag{3}$$

and thereby an additional constraint $\sum_{t=1}^{T} P_{j,t}^{\mathrm{EV}} \cdot \Delta t \ge E_j^r$ should be imposed. However, this requirement may not be satisfied during disruptive events, since a resilient MEMG tends to prioritize the supply of essential loads with limited local resources, which may compromise EVs' benefits.

2.3. Aggregate demand

In the case where local load curtailment is inevitable when island mode is enforced, it is important to differentiate the supply priority of different types of load in order to alleviate the adverse impacts on local communities. In this work, various electricity loads are categorized into three types, comprising essential load, non-essential load and EV charging load. Essential load is typically related to basic societal functions. The maintenance of essential load during disruptive events is the key objective of resiliency-oriented operation of MEMG and should be prioritized above all. The uninterrupted supply of non-essential load should be secured in normal situations under the framework of power system security and reliability. However, during HILP disruptive events, the supply of non-essential loads should be strategically compromised for the survival of essential load, thus fulfilling the aim of resilience enhancement.

Let us denote the essential and non-essential load of MEMG m at time t by $D_{m,t}^{\mathrm{EL}}$ and $D_{m,t}^{\mathrm{NEL}}$ respectively. Then, in combination with EV power exchange, the aggregate electricity demand of MEMG m at time t is expressed as

$$D_{m,t} = D_{m,t}^{\mathrm{EL}} + D_{m,t}^{\mathrm{NEL}} + \sum_{j \in \mathcal{N}_m} P_{j,t}^{\mathrm{EV}}. \tag{4}$$

Accordingly, the total demand of the MEMG cluster follows

$$D_t = \sum_{m \in \mathcal{M}} D_{m,t}^{\mathrm{EL}} + \sum_{m \in \mathcal{M}} D_{m,t}^{\mathrm{NEL}} + \sum_{m \in \mathcal{M}} \sum_{j \in \mathcal{N}_m} P_{j,t}^{\mathrm{EV}}, \tag{5}$$

2.4. optimisation framework

The objective of the resiliency-oriented V2G scheduling is to minimise the local load curtailment of the MEMG during disruptive events with the lowest economic costs. Based on the architecture of the MEMG cluster in Section 2.1, the optimal energy resource allocation, for MEMG $m \in \mathcal{M}$, interconnection line $n \in \mathcal{L}(m)$, and EV $j \in \mathcal{N}$ at time $t \in \mathcal{T}$, is determined by the following optimisation problem

$$\begin{aligned}\min_{\Xi} \quad C_{\mathrm{Total}} = \sum_{t=0}^{T} \sum_{m=1}^{M} \Big(& f_m(P_{m,t}^{\mathrm{RE}}) + c_{m,t}^{\mathrm{CG}} \cdot P_{m,t}^{\mathrm{CG}} + (1 - I_t^{\mathrm{HILP}}) \cdot c_{m,t}^{\mathrm{UG}} \cdot P_{m,t}^{\mathrm{UG}} \\ & + \sum_{k \in \{\mathrm{EL,\ EV,\ NEL}\}} I_t^{\mathrm{HILP}} \cdot \tilde{C}_{m,t}^{k} \Big)\end{aligned} \tag{6}$$

$$s.t.\ P_{m,t}^{\mathrm{RE}} + P_{m,t}^{\mathrm{UG}} + P_{m,t}^{\mathrm{CG}} + C_{m,n,t}^{\mathrm{L}} = D_{m,t}, \tag{6a}$$

$$0 \le P_{m,t}^{\mathrm{UG}} \le (1 - I_t^{\mathrm{HILP}}) \cdot \overline{P}_m^{\mathrm{UG}}, \tag{6b}$$

$$0 \le P_{m,t}^{\mathrm{RE}} \le \overline{P}_{m,t}^{\mathrm{RE}}, \tag{6c}$$

$$0 \le P_{m,t}^{\mathrm{CG}} \le \overline{P}_{m,t}^{\mathrm{CG}}, \tag{6d}$$

$$-\overline{C}_{m,n}^{\mathrm{L}} \le C_{m,n,t}^{\mathrm{L}} \le \overline{C}_{m,n}^{\mathrm{L}}, \tag{6e}$$

$$P_j^{\mathrm{EV}} \in \mathcal{P}_j^{\mathrm{EV}}, \tag{6f}$$

$$(1 - I_t^{\mathrm{HILP}}) \cdot \left(E_j^r - \sum_{t \in \mathcal{A}_j} P_{j,t}^{\mathrm{EV}} \cdot \Delta t \right) \leq 0, \tag{6g}$$

where $\Xi = \{P^{\mathrm{RE}}, P^{\mathrm{UG}}, P^{\mathrm{CG}}, P^{\mathrm{EV}}, C^{\mathrm{L}}\}$ denotes the set of decision variables. The objective function C_{Total} comprises the operational cost and the penalty cost (incurred by load curtailment in contingencies). The operational mode of the MEMG is indicated by the binary parameter I_t^{HILP}, i.e., $I^{\mathrm{HILP}} = 0$ for normal mode and $I^{\mathrm{HILP}} = 1$ for island mode. Under either mode, the power balance should fulfil equality (6a). The power supplies from the utility grid, local RES and controllable generators as well as interconnection between different MEMGs are constrained by (6b)-(6e). Meanwhile, EV power exchange should follow (6f). Regarding constraint (6g), the energy demand of EV population has to be satisfied during normal operational mode. However, if a disruptive event occurs, the supply of essential load curtailment is prioritized in which case (6g) can be violated with penalty.

It is noticed that the optimisation problem (6) has numerous decision variables due to the involvement of EV participants and the objective function accounting for the cost over a large scale system is not linear. Together with the fact that knowing the specific parameters of each EV by a central controller is not practical, a distributed optimisation approach that each EV optimises its individual operational schedule is preferable. Before the distributed optimisation approach, the formulations of total cost, RES curtailment, and load curtailments in the two operational modes are defined.

Normal operation: In normal operational conditions, the MEMG is connected to the utility grid, where local electricity demand can be supplied by both the utility grid and local energy sources. Meanwhile, EVs are assumed to follow an economy-oriented charging pattern. As a result, the cost at normal operation time t is the objective function (6) when $I_t^{\mathrm{HILP}} = 0$ and it is expressed as

$$\sum_{m=1}^{M} \left(f_m(P_{m,t}^{\mathrm{RE}}) + c_{m,t}^{\mathrm{UG}} \cdot P_{m,t}^{\mathrm{UG}} + c_{m,t}^{\mathrm{CG}} \cdot P_{m,t}^{\mathrm{CG}} \right) \tag{7}$$

where the three terms are the penalized cost of RES curtailment, electricity purchase cost and local generation cost, respectively. Particularly, the penalty function is expressed as

$$f_m(P_{m,t}^{\mathrm{RE}}) = \frac{1}{2} \alpha_m^{\mathrm{RE}} \cdot (\overline{P}_{m,t}^{\mathrm{RE}} - P_{m,t}^{\mathrm{RE}})^2 \tag{8}$$

where α_m^{RE} is a positive coefficient.

The system operator then solves the optimisation problem (6) and broadcasts the marginal cost as a common signal to coordinate the power exchange of various EVs. Individual EVs respond to this common signal by adjusting their power exchange schedule in an organised way to further reduce the total cost C_{Total}. Details in this process will be elaborated in Section 3. Although the impact of a single EV response on the marginal cost signal is minor, collective response of numerous EVs can make a fundamental difference. Therefore, it is necessary to quantify the sensitivity of cost C_{Total} in normal mode with respect to the power profile P_j^{EV} of a single EV by calculating the following gradient

$$\lambda_m^{\mathrm{NM}} = \nabla_{P_j^{EV}} C_{\mathrm{Total}} = \left[\frac{\partial C_{\mathrm{Total}}}{\partial P_{j,1}^{EV}}, \frac{\partial C_{\mathrm{Total}}}{\partial P_{j,2}^{EV}}, \cdots, \frac{\partial C_{\mathrm{Total}}}{\partial P_{j,T}^{EV}} \right] \tag{9}$$

In particular, the marginal cost $\lambda_{m,t}^{\mathrm{NM}} = \frac{C_{\mathrm{Total}}}{\partial P_{j,t}^{EV}}$, is determined by the dual variable of power balance constraint (6a) at node m and time t.

Island mode: When a contingency occurs and leads to the failure of partial generation/transmission capacities of the power system, MEMG can operate in island mode, thus mitigating the supply pressure of the main grid. However, local electricity demand can only be supplied by local energy sources and is under significant risks of being curtailed. In this case, EVs can be called to adjust their power exchange schedules for resilience enhancement, but potentially at the cost of jeopardising their own interests. In this case, EV load curtailment is defined as the gap between the required energy level and the energy level at departure, i.e., $\left(SOC_j^r - SOC_{j,t_j^{out}} \right) \cdot \bar{E}_j$. Therefore, the total EV load curtailment of MEMG m at any particular time t is calculated as

$$Cur_{m,t}^{\mathrm{EV}} = \sum_{j : t_j^{out} = t} \left(SOC_j^r - SOC_{j,t} \right) \cdot \bar{E}_j. \tag{10}$$

Meanwhile, the essential and non-essential load curtailments are determined by

$$Cur_{m,t}^{\mathrm{EL}} = \left[D_{m,t}^{\mathrm{EL}} - P_{m,t}^{\mathrm{CG}} - P_{m,t}^{\mathrm{RE}} + \left[\sum_{j \in \mathcal{N}_m} P_{j,t}^{\mathrm{EV}} \right]^- \right]^+ \tag{11a}$$

$$Cur_{m,t}^{\mathrm{NEL}} = \left[D_{m,t}^{\mathrm{NEL}} - \left[P_{m,t}^{\mathrm{CG}} + P_{m,t}^{\mathrm{RE}} - D_{m,t}^{\mathrm{EL}} - \left[\sum_{j \in \mathcal{N}_m} P_{j,t}^{\mathrm{EV}} \right]^+ \right]^+ \right]^+ \tag{11b}$$

where operator $[\cdot]^{+/-} = \max / \min\{\cdot, 0\}$ indicates taking the maximum/minimum value between $\cdot$ and 0. Then, with the calculated amount of energy curtailment, the corresponding penalty cost, i.e., $\tilde{C}_m^{\mathrm{EL}}$ for essential load curtailment, $\tilde{C}_m^{\mathrm{EV}}$ for EV load curtailment, and $\tilde{C}_m^{\mathrm{NEL}}$ for non-essential load curtailment, are defined as

$$\tilde{C}_{m,t}^k = \frac{1}{2} \alpha_m^k \cdot (Cur_{m,t}^k)^2 + \beta_m^k \cdot Cur_{m,t}^k \tag{12}$$

where $k \in \{\mathrm{EL}, \mathrm{EV}, \mathrm{NEL}\}$. α_m^k and β_m^k are penalty coefficients, the values of which are selected based on the criticality of the corresponding load.

Now, the total cost when the MEMG is in island mode can be formulated as (13). Compared to the total cost in normal mode as shown in (7), the RES curtailment penalty cost and the local generation cost remain the same but the electricity purchase cost is removed because the MEMG is disconnected from the utility grid. Moreover, when the power supply cannot meet the demand during the contingency, the penalty terms regarding the essential load curtailment, EV energy curtailment, and the non-essential load curtailment are appended to the cost function with different weighting parameters indicating different priority.

$$\sum_{m=1}^{M} \left(f_m(P_{m,t}^{\mathrm{RE}}) + c_{m,t}^{\mathrm{CG}} \cdot P_{m,t}^{\mathrm{CG}} + \sum_{k \in \{\mathrm{EL},\ \mathrm{EV},\ \mathrm{NEL}\}} \tilde{C}_{m,t}^k \right) \tag{13}$$

To capture the marginal cost in island mode, the gradient of the total cost C_{Total} with respect to the power exchange schedule of EV j at MEMG m is calculated which is in the same form of (9) and denoted by λ_m^{IM}. Given the marginal cost of normal operation mode λ_m^{NM} and the marginal cost of island mode λ_m^{IM}, the key information that is used to coordinate the dispatch of numerous EVs is calculated as

$$\lambda_{m,t} = (1 - I_t^{\mathrm{HILP}}) \cdot \lambda_{m,t}^{\mathrm{NM}} + I_t^{\mathrm{HILP}} \cdot \lambda_{m,t}^{\mathrm{IM}} \tag{14}$$

which will be used to guide the resiliency-oriented adjustment of EV power exchange in Section 3.

3. Distributed control strategy for an individual MEMG

During disruptive events, EVs can adjust their original power exchange plans in a resiliency-oriented way. To mitigate load curtailment, particularly in respect of essential load, a distributed rescheduling strategy for the operation of numerous EVs is introduced in this section. Specifically, a sequential iterative algorithm is proposed to collectively coordinate the resiliency-oriented rescheduling of multiple EVs, where each EV follows a multi-phase adjustment strategy, as demonstrated in Fig. 3. Phase 1 aims to reduce essential load curtailment, while Phase 2 is motivated by satisfying EV energy requirements at departure. Finally, the mitigation of non-essential load curtailment is focused. Note that the order of the three phases corresponds to the priority list of different loads.

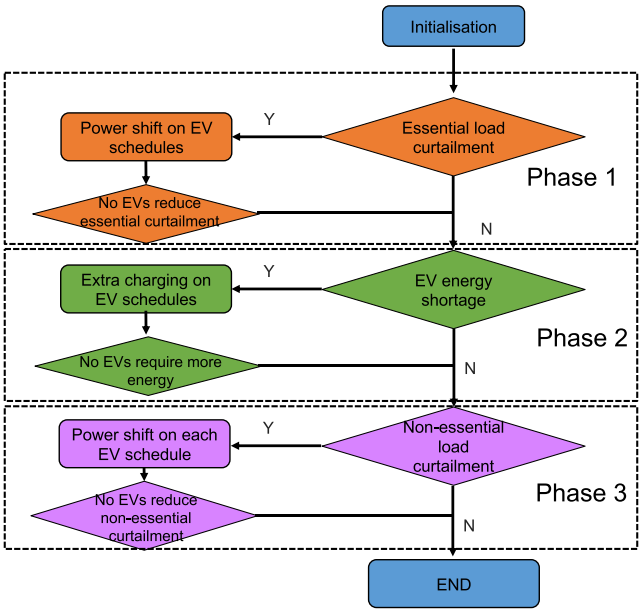

Fig. 3. Flow chart of the multi-phase algorithm.

3.1. Phase 1: Power shifting for essential load shedding

Motivated by alleviating essential load curtailment, for EV j, an amount of power, i.e., $\delta_1 > 0$, is shifted from time $\underline{t} \in \mathcal{A}_j$ to time $\overline{t} \in \mathcal{A}_j$. Starting from an initial power exchange profile $P_j^{\mathrm{EV}} \in \mathcal{P}_j^{\mathrm{EV}}$, the adjusted profile $P_j^{\mathrm{EV},+}$ after power shift is formulated as Equation (15):

$$P_{j,s}^{\mathrm{EV},+} = \begin{cases} P_{j,s}^{\mathrm{EV}} - \delta_1 & \text{if } s = \underline{t} \\ P_{j,s}^{\mathrm{EV}} + \delta_1 & \text{if } s = \overline{t} \\ P_{j,s}^{\mathrm{EV}} & \text{otherwise} \end{cases} \tag{15}$$

The power shift operation, i.e., $\delta_1(\underline{t}, \overline{t})$ is determined as follows:

3.1.1. Feasible magnitude of shifted power

For an initial power exchange schedule of EV j, i.e., $P_j^{\mathrm{EV}} \in \mathcal{P}_j^{\mathrm{EV}}$, the amount of power δ_1 that can be shifted is limited by the quantity $\overline{\delta}_1$, defined in Equation (16):

$$\begin{aligned} \overline{\delta}_1 = \min\{ & a_1(P^{\mathrm{EV}}, j, \overline{t}), b_1(P^{\mathrm{EV}}, j, \underline{t}), c_1(P^{\mathrm{EV}}, j, \underline{t}, \overline{t}), \\ & d_1(P^{\mathrm{EV}}, j, \overline{t}), e_1(C^{\mathrm{L}}, P^{\mathrm{EV}}, j, \underline{t}, \overline{t})\}. \end{aligned} \tag{16}$$

Each term of the minimum function in (16) is specified as:

- *maximum feasible power increase* at time $\overline{t}$:

$$a_1(P^{\mathrm{EV}}, j, \overline{t}) = \overline{P}_j^{\mathrm{EV}} - P_{j,\overline{t}}^{\mathrm{EV}} \tag{17}$$

- *maximum feasible power decrease* at time $\underline{t}$:

$$b_1(P^{\mathrm{EV}}, j, \underline{t}) = P_{j,\underline{t}}^{\mathrm{EV}} - \underline{P}_j^{\mathrm{EV}} \tag{18}$$

- *Maximum feasible power shift* that fulfils energy limits:

$$c_1(P^{\mathrm{EV}}, j, \underline{t}, \overline{t}) = \begin{cases} \min_{t \in \{\underline{t}, \cdots, \overline{t}-1\}} \frac{\bar{E}_j \cdot \left(SOC_{j,t} - \underline{SOC}_j \right)}{\Delta t} & \text{if } \underline{t} < \overline{t} \\ \frac{\bar{E}_j \cdot \left(\overline{SOC}_j - \min_{t \in \{\overline{t}, \cdots, \underline{t}-1\}} SOC_{j,t} \right)}{\Delta t} & \text{if } \underline{t} > \overline{t} \end{cases} \tag{19}$$

- *Maximum feasible power shift* that fulfils local network capacity limits:

$$d_1(P^{\mathrm{EV}}, j, \overline{t}) = \overline{D}_m - D_{m,\overline{t}} \tag{20}$$

- *Maximum feasible power shift* that fulfils interconnection line capacity limits:

$$e_1(C^{\mathrm{L}}, P^{\mathrm{EV}}, j, \overline{t}, \underline{t}) = \overline{C}_{m,n}^{\mathrm{L}} - C_{m,n,\tau}^{\mathrm{L}}, \quad \text{if } \tau \in \{\overline{t}, \underline{t}\} \tag{21}$$

Constraints (17) and (18) ensure EV power exchange is always within its physical limits $[\underline{P}_j^{\mathrm{EV}}, \overline{P}_j^{\mathrm{EV}}]$, while Constraint (19) guarantees the SOC at any time would not exceed the upper and lower bounds. By imposing (20), the local distribution capacity is taken into account while implementing power shift across numerous EVs to avoid overloading local networks. Moreover, the interaction between different MEMGs is restricted by the interconnection capacity, as shown in (21).

3.1.2. Selection of shifting time pair

While selecting the optimal time instants to implement the power shift, the following two factors should be considered.

– DN congestion management:

To ensure that the aggregate demand in each individual MEMG does not exceed the local network capacity, Constraint (22) should be satisfied:

$$D_{m,t} = D_{m,t}^{\mathrm{EL}} + D_{m,t}^{\mathrm{NEL}} + \sum_{j \in \mathcal{N}_m} P_{j,t}^{\mathrm{EV}} \leq \overline{D}_m. \tag{22}$$

Specifically, if condition (22) is violated, it is necessary for EVs to shave the peak demand by reducing charging power or increasing discharging power. In particular, each EV in this MEMG checks its availability at the network-overloaded time $\underline{t}^\star$ and respond accordingly to shave demand, i.e.,

$$\underline{t}^\star \in \underset{t \in \mathcal{A}_j : D_{m,t} > \overline{D}_m}{\operatorname{argmax}} D_{m,t}. \tag{23}$$

After selecting time instant $\underline{t}^\star$, the associated optimal $\overline{t}^\star$ is calculated as follows

$$\overline{t}^\star \in \underset{\substack{t \in \mathcal{A}_j \,:\, D_{m,t} < \overline{D}_m \\ \bar{\delta}_1(P^{\mathrm{EV}}, j, \underline{t}^\star, t) > 0}}{\operatorname{argmin}} \lambda_t, \tag{24}$$

which aims at minimizing the cost increase incurred by network congestion alleviation.

Through the selection of time pair $(\underline{t}^\star, \overline{t}^\star)$ as in (23) and (24) with the magnitude determined by (16), the power shift operation $\delta_1(\underline{t}, \overline{t})$ reduces local peak demand in the most economic manner. Therefore, sequentially updating the power exchange of different EVs can cost-effectively realise network congestion management.

– Resilience-driven energy arbitrage:

Since the primary goal of this algorithm is to enhance system resilience, power shift should be then driven by reducing the attached costs of penalizing essential load curtailment. Specifically, a certain amount of electricity power is charged to EVs at time instants with low marginal penalized cost and released when marginal penalized cost is high. This service can be implemented through multiple steps of power shift. In each step, the power shift δ_1 from $\underline{t}$ to $\overline{t}$ would lead to reduction in curtailment-related penalized costs. To obtain the most significant cost reduction in a single step of power shift, the optimal $(\underline{t}^\star, \overline{t}^\star)$ are identified according to

$$(\underline{t}^\star, \overline{t}^\star) \in \underset{(\underline{t}, \overline{t}) \in \mathcal{A}_j \times \mathcal{A}_j}{\operatorname{argmin}} (\lambda_{\overline{t}} - \lambda_{\underline{t}}) \cdot \bar{\delta}_1(P^{\mathrm{EV}}, j, \underline{t}, \overline{t}). \tag{25}$$

3.2. Phase 2: EV energy compensation

The process of EV power shift in Phase 1 is dedicated to reducing essential load curtailment, disregarding EVs' own interests. This can lead to a situation where EVs are not charged to their required energy level at departure. To address this issue, this phase aims to fill the gap between

the SOC after EV providing the service in Phase 1 and the required SOC at departure. This is implemented by using the available local energy sources at this stage, i.e., the energy that can be delivered for EV energy compensation must be from either unused local RES and controllable generation or those have been supplied to non-essential load. To fulfil this purpose, the following steps will be carried out:

– Priority sorting for EV charging:

Since different EVs are characterized by customized trip schedules, it is imperative to sort the suitability of individual EVs providing V2G services by taking into account the temporal and spatial availability of numerous EVs. To this end, two indices proposed in [40] are adopted to sort the priority of EV charging, namely the response time margin (RTM) and the state of charge margin (SOCM). Specifically, RTM, which describes the maximum time an EV stays connected to the system, is defined as

$$RTM_j = t_j^{out} - t_j^{in}. \tag{26}$$

The smaller RTM_j is, the shorter charging time that the EV can sustain. This means that an EV with smaller RTM_j is expected to be selected with a high priority for charging. However, at a particular time instant, there may be multiple EVs with the same RTM. Therefore, the other index SOCM, expressed as below, needs to be employed

$$SOCM_j = \max\{0, SOC_j^r - SOC_{j,t_j^{in}}\}. \tag{27}$$

The greater SOCM is, the higher charging urgency will be. Therefore, EVs with greater SOCM and smaller RTM are prioritized to be compensated.

Based on these two indices, an integrated parameter, which is defined as the response margin ratios (RMR), viz,

$$RMR_j = \frac{SOCM_j}{RTM_j} \tag{28}$$

is used as the criterion to determine the orders of EVs for energy compensation. According to the above analysis that both the greater SOCM and smaller RTM will prioritize the EV for charging, the principle to select EV in Phase 2 follows a descending order of the RMR. Notice that this order is updated once an EV finishes its rescheduling and the available participant with the lowest ROM could implement the charging for energy compensation consecutively.

– Maximum power compensation:

After the MEMG is disconnected from the utility grid, EVs, which have not been charged to their required energy level, would expect additional energy from controllable generation. As the essential load demand has higher priority relative to the EVs, it is not convenient to charge EVs while sacrificing essential demand supply. Hence, the energy that can be delivered for EV energy complement must be from either unused local generation or those have been supplied to non-essential load.

No matter which source that the energy comes from, the additional power that can be added to the EV operation schedule is restricted by the quantity $\overline{\delta}_2$ which is defined as:

$$\overline{\delta}_2(P^{\mathrm{EV}}, j, t_0) = \min\{a_2(P^{\mathrm{EV}}, j, t_0), b_2(P^{\mathrm{EV}}, j, t_0), c_2(P^{\mathrm{EV}}, j, t_0)\}. \tag{29}$$

Each term of the function in (29) is specified as:

- *maximum feasible power increase* at time t_0:

$$a_2(P^{\mathrm{EV}}, j, t_0) = \overline{P}_j^{\mathrm{EV}} - P_{j,t_0}^{\mathrm{EV}} \tag{30}$$

- *Maximum feasible power swap* that fulfils energy constraints after t_0:

$$b_2(P^{\mathrm{EV}}, j, t_0) = \frac{\bar{E}_j \cdot \left(\overline{SOC}_j - \min_{t>t_0} SOC_{j,t}\right)}{\Delta t} \tag{31}$$

- *Maximum feasible power increase* that fulfils local capacity constraints:

$$c_2(P^{\mathrm{EV}}, j, t_0) = \overline{D}_m - D_{m,t_0} \tag{32}$$

Similar to the upper bounds (17), (19) and (20) in Phase 1, the bounds in (30), 31 and (32) are imposed to ensure the EV operation schedule fulfills its operational conditions and the local capacity.

After considering the maximum convenient charging power at each time instant within the EV's availability window, the next step is to determine the optimal reschedule among all these potential options. Considering time instants with electricity supply surplus, if there are EVs which are available for power increase at these time instants, their optimal options could be charging as much as possible because the price is relatively low compared to charge by curtailing the non-essential demand. However, if there is no power surplus within some EVs' availability window, their energy level increment can only be achieved by scarifying non-essential load and inducing penalty because of the priority. Overall, in order to charge the EV for energy complement with a low cost, the optimal time instant is identified by

$$t_0^{\star} \in \underset{\tau \in \mathcal{A}_j}{\operatorname{argmin}} \ \lambda_\tau \cdot \overline{\delta}_2(P^{\mathrm{EV}}, j, \tau). \tag{33}$$

Through iterative energy compensation on all EVs, the total energy curtailment at their departure time can be minimised.

3.3. Phase 3: Power shifting for non-essential load shedding

After completing the power shift for essential load curtailment minimisation and the extra charging for EV energy shortage, EV flexibility can be also used to reduce the non-essential load curtailment. Similar to the restrictions in (16) for essential load, the maximum power shift for non-essential load is also bounded by

$$\overline{\delta}_3(P^{\mathrm{EV}}, j, \underline{t}, \bar{t}) = \min\{a_3(P^{\mathrm{EV}}, j, \bar{t}), b_3(P^{\mathrm{EV}}, j, \underline{t}), c_3(P^{\mathrm{EV}}, j, \underline{t}, \bar{t}), d_3(P^{\mathrm{EV}}, j, \bar{t})\}. \tag{34}$$

where a_3, b_3, c_3, d_3 are following the same expressions in (17), (18), (19) and (20), respectively.

3.4. Iterative control algorithm

Due to the limited capacity and minor market power of each EV, as depicted in Fig. 4, aggregators are typically used to exchange electricity between EVs and the power grid. With the distributed control framework where each EV operates independently in response to marginal cost signals, the proposed approach boils down the complex task of coordinating large systems with large population of participants into smaller sub-problems.

The EV coordination strategy basically incorporates 4 steps:

Step 1: Without loss of generality, the operational schedule of all EVs before the disruptive events is initialised to be the same as their original charging plan, whereas the EVs status are set to be idle (no charging and discharging) after the event. Individual EVs submit their initial electricity demand profiles to the aggregator. Based on the aggregate EV power, the central unit minimises the objective function (6) subject to constraints (6a)-(6e) and (4). Then, the initial marginal cost λ_m is evaluated according to (14) and the congestion information of the interconnection lines is obtained according to the optimisation solution.

Step 2: EV j receives the marginal signal and congestion information to minimise the load curtailment by updating its operational profiles through power shifting approach under the three-phase control framework. Then, the adjusted charging/discharging schedule is submitted to the aggregator.

Step 3: The central unit revises the aggregate electricity demand of EV population and minimises the objective function (6) subject to constraints (6a)-(6e) and (4) again to update the marginal cost signal λ_m. Then, EV $j+1$ receives the associated updated marginal cost and congestion state.

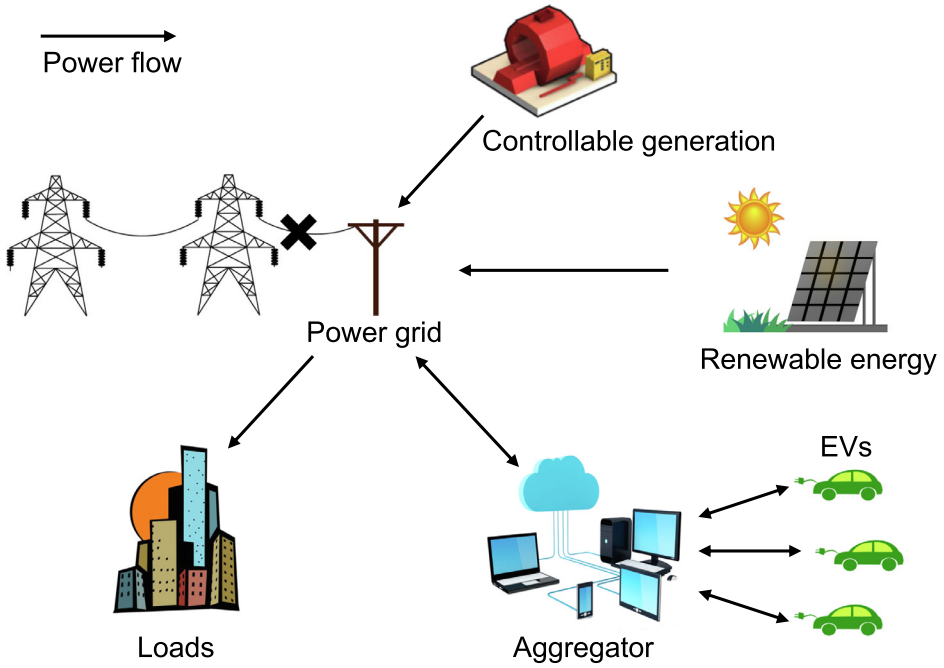

Fig. 4. Power exchange between EVs and the power grid.

Step 4: Repeat Step 2 and 3 until the convergence condition, that no EV can achieve further total cost reduction by unilaterally changing its charging/discharging operation profile, is satisfied.

The iterative coordination process is performed day-ahead. It links the global interest with the individual EV charging/discharging behaviour. From the system perspective, the system operator aims to minimise the load curtailment as formulated in the objective function of (6). From the EV perspective, based on the global marginal cost, the customers provide V2G service to minimise the essential/non-essential load curtailment and seek for individual energy compensation taking advantage of its flexibility. Since EVs only inform the aggregator of the amount of electricity energy they required, other information such as EV parameters and travelling behaviour are not leaked, thereby the customer privacy is protected.

Next, the convergence of iterative control algorithm will be analysed. Let us first consider the power shift $\delta > 0$ in either Phase 1 or Phase 3 of an arbitrary iteration ℓ from $\underline{t}^\star$ to $\overline{t}^\star$, the total demands that are the sum of the essential, non-essential load, and the EV aggregator at these two instants fulfil the following equations

$$D^{(\ell)}_{\overline{t}^\star} - D^{(\ell-1)}_{\overline{t}^\star} = \delta, \quad D^{(\ell)}_{\underline{t}^\star} - D^{(\ell-1)}_{\underline{t}^\star} = -\delta. \tag{35}$$

Since the objective function C_{Total} in (6) can be formulated as a quadratic function with respect to the total demand, the variation of C_{Total} by performing the power shift at iteration ℓ can be explicitly derived as

$$\begin{aligned} C_{\text{Total}}(D^{(\ell)}) - C_{\text{Total}}(D^{(\ell-1)}) &\approx \lambda_{\underline{t}^\star}(D^{(\ell)}_{\underline{t}^\star} - D^{(\ell-1)}_{\underline{t}^\star}) + \lambda_{\overline{t}^\star}(D^{(\ell)}_{\overline{t}^\star} - D^{(\ell-1)}_{\overline{t}^\star}) \\ &= \lambda_{\underline{t}^\star} \cdot (-\delta) + \lambda_{\overline{t}^\star} \cdot \delta \\ &= \delta(\lambda_{\overline{t}^\star} - \lambda_{\underline{t}^\star}) \le 0, \end{aligned} \tag{36}$$

where the last inequality holds because the power shift is implemented from the high marginal cost time instant $\underline{t}^\star$ to the low marginal cost time instant $\overline{t}^\star$, i.e., $\lambda_{\overline{t}^\star} \le \lambda_{\underline{t}^\star}$. As a result, equation (36) yields a reduction of total cost by performing power shift. Additionally, in Phase 2 aiming at EV energy compensation, the charging operation for EV batteries will decrease the total cost because the EV energy curtailment has the highest penalty after Phase 1. Overall, the iterative control algorithm ensures the convergence until no EV can further reduce the total cost by unilaterally changing its charging/discharging operation profile.

Table 1
Parameters for the EV population

Parameter	Mean	Std	Parameter	Mean	Std
$\overline{P}^{\text{EV}}_j, \underline{P}^{\text{EV}}_j$	5 kW	0.5 kW	$\tilde{E}_j$	20 kWh	2 kWh
SOC_{j,t^{in}_j}	0.5	0.05	SOC^r_j	0.8	0
$\overline{SOC}_j$	1	0	$\underline{SOC}_j$	0.2	0

4. Numerical results

4.1. Assumptions and parameters

The performance of the distributed coordination strategy is evaluated in this section through a series of case studies on a single MEMG and a system of three MEMGs. Simulations are conducted in Matlab R2019a, over a 24-hour time horizon from 12:00 PM to 12:00 PM in the next day, with the sampling period of 15 min. The occurrence time of contingency is assumed to be at 6:00 AM. The computation hardware is a laptop with 2-core 3.50GHz processor and 32GB RAM.

Regarding the parameters of the single MEMG system, the essential and non-essential demand profiles have been chosen as shown in Fig. 5. The maximum power supply from utility grid is $\overline{P}^{\text{UG}} = 20$ MW. The electricity price of using controllable generators is fixed at $c^{\text{CG}} = 225$ £/MWh and the maximum output power is $\overline{P}^{\text{CG}} = 4$ MW.

In this MEMG system, a population of $N = 1000$ EVs participating in the resilience enhancement service has been considered. The relevant parameters of EVs are following Gaussian distribution with the mean and standard deviation in TABLE 1. The plug-in and plug-out time are generated based on the multimodal normal distribution functions in [41].

Note that the novel algorithm in this paper has no requirement for the parameters. In practice, the EV parameters such as charging/discharging power and battery capacity may be more diversified and lead to different numerical results. Nevertheless, the superior performance in resilience enhancement and computational burden reduc-

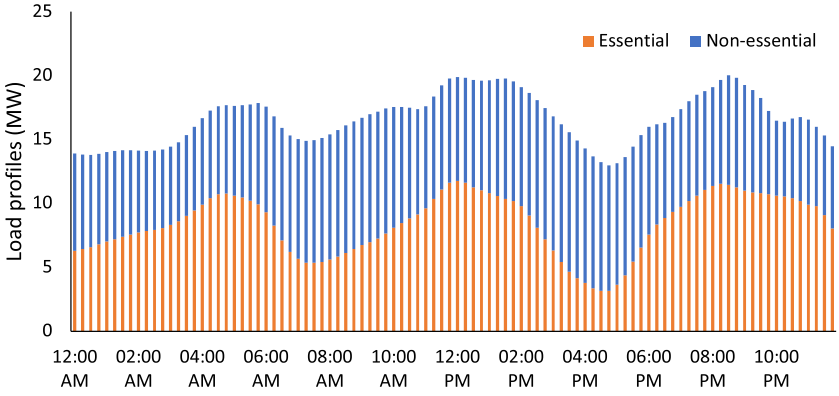

Fig. 5. Essential and non-essential load profiles.

tion will be effectively preserved due to the distributed characteristic of the iterative approach.

Next, some case studies are conducted to demonstrate the advantages of proposed control strategy.

4.1.1. Smart load curtailment management

Instead of the commonly used linear penalty function for load curtailment in the literature, the penalty function is defined as a quadratic form in (12). To demonstrate the benefits of smart load curtailment management technique by using the quadratic functions, the following two cases are compared.

- *Case 1-A*: The load curtailment penalty functions are linear functions with constant coefficients, i.e., $\alpha^k = 0$ for $k \in \{\text{EL}, \text{NEL}\}$ and $\beta^{\text{EL}} = 10000, \beta^{\text{NEL}} = 100$.
- *Case 1-B*: The load curtailment penalty functions are modelled as quadratic functions, i.e., $\alpha^{\text{EL}} = 20000, \beta^{\text{EL}} = 10000$, and $\alpha^{\text{NEL}} = 200, \beta^{\text{NEL}} = 100$.

The energy supply and demand profiles are shown in Fig. 6. In both cases, it can be seen that the combined power supply of utility grid and controllable generation is sufficient to meet the total demand before the disruptive event. While the disruptive event occurs, the energy sources are managed to supply the essential load. Specifically, the essential load curtailment between 6:00 AM and 9:00 AM has been compensated by the V2G service. Then, EVs are charged during 9:00 AM - 5:00 PM when PV is available, and the charged energy is released to mitigate the essential load curtailment after 5:00 PM. In this regard, the resiliency of the MEMG system has been tremendously enhanced.

Compared to Case 1-A, the penalty model in Case 1-B provides a smooth essential load curtailment as shown in Fig. 6. By using the quadratic penalty function, the marginal cost is proportional to the amount of essential load curtailment. Thus, the time instants with higher essential load curtailment are more likely to be compensated by discharging EVs. Thanks to the employment of this smart load curtailment management technique, the imbalance between demand and supply does not experience major fluctuations, which effectively mitigates the threats to the operation stability of the MEMG. Furthermore, the smart load management approach in Case 1-B results in 6.89 MWh total essential load curtailment that is 30.8% less than 9.95 MWh in Case 1-A. This is because the power shifting by each EV to compensate the essential load curtailment in Case 1-B provides higher flexibility. Specifically, the criterion to select discharging time in Case 1-B when an EV performs its power shifting is to minimise the highest essential load curtailment, whereas Case 1-A may always choose the earliest time of non-zero essential load curtailment. As a result, in Case 1-B, more EVs with earlier departure time can also participate in the V2G service and provide flexibility to reduce the essential load curtailment.

Table 2
Computational performance and Optimality

Number of EVs		10	100	1000	10000
Centralised	Time (sec)	1.95	13.90	925.04	N.A.
	Curtail (MWh)	40.61	31.40	9.42	N.A.
Distributed	Time (sec)	2.39	18.14	121.82	302.42
	Curtail (MWh)	40.67	31.53	9.95	0

4.1.2. Computational performance and optimality

To evaluate the computational performance of the proposed coordination method, the simulation time and the essential load curtailment at different number of EVs are compared with the centralised optimisation-based approach. The simulation results are shown in Table 2.

It can be seen that the computational advantage of the distributed method increases exponentially compared to the centralised optimisation with the increase of the EV number, although the optimality in essential load curtailment is slightly lost. Specifically, for the centralised method, the computational time is increasing dramatically with respect to the growth of EV number. In particular, when the EV number is increased to 10000, the centralised approach is not available (N.A.) for computation because the corresponding optimisation problem is not able to provide a solution after many hours. Regarding the distributed method, the computational speed is much faster when numerous EVs are participating the resilience optimisation, and thereby indicating feasibility to the adoption of rolling horizon framework.

Moreover, in Table 2, a downwards trend in essential load curtailment is observed with the increasing number of EVs because more flexibility are provided to temporally shift local generation under the situation of severe essential load curtailment. This result further indicates the benefits of deep electrification in the transport sector to potentially provide huge amount of flexibility and resiliency for the power system. For the scenarios with same EV number, it is observed that the differences on essential load curtailment between the centralised and the distributed optimisation methods are minor, so the significant improvement on computational speed for large scale optimisation problem using the distributed approach does not impose much scarification on resilience optimality.

4.2. Multiple MEMGs

Next, let us consider a power system with three MEMGs, $m = \{1, 2, 3\}$, interconnected with each other where the unused PV, CG, utility grid and EV energy can be transmitted to other MEMGs to mitigate the load curtailment. The number of EVs in these MEMGs are $N_1 = 2000$, $N_2 = 1000$ and $N_3 = 3000$, respectively. The parameters of EVs follow the same distribution as described in TABLE 1. The total electricity de-

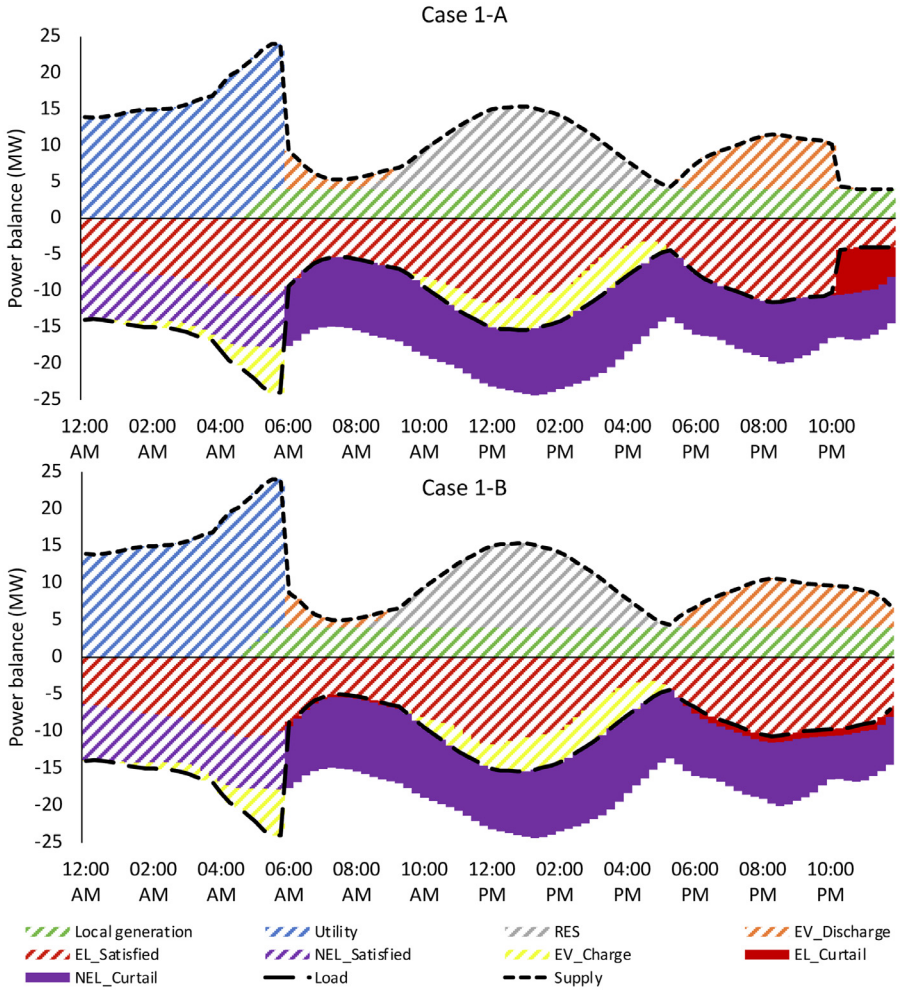

Fig. 6. Essential load curtailment with/without smart load curtailment management.

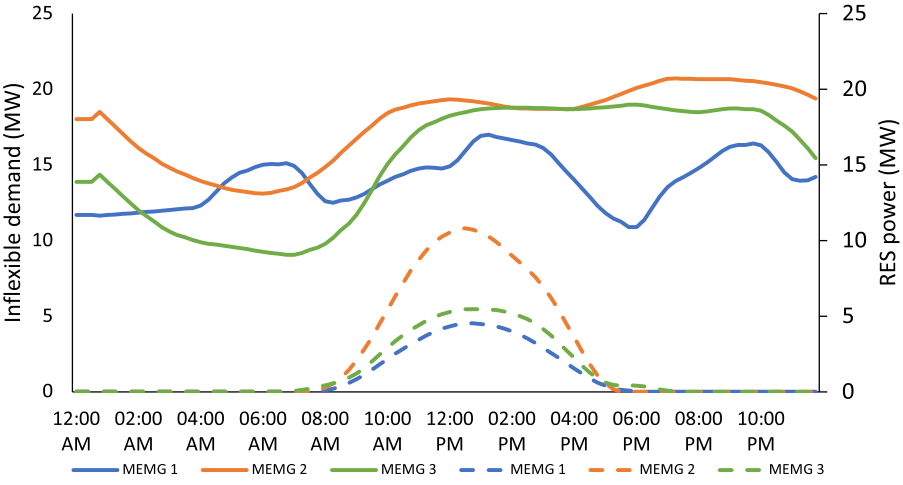

Fig. 7. Total electricity demand (solid lines) and maximum RES power (dashed lines) of the three MEMGs.

mand and available RES profiles are depicted in Fig. 7. Other relevant parameters are shown in TABLE 3. The penalty parameters for these three MEMGs are assumed to be the same.

Fig. 8 shows the four types of coordinated operation for the power exchange between MEMGs. Type 1 represents the standard demand shift operation within a single MEMG system utilising the EV temporal flexibility. Due to the uneven distribution of the local resources and the flexibility in different regions, EVs can also provide spatial flexibility through the interconnection between any two MEMGs as represented

Table 3
Parameters for the EV population

	Value		Value		Value
$\overline{P}_1^{UG}$	20 MW	$\overline{P}_2^{UG}$	20 MW	$\overline{P}_3^{UG}$	20 MW
$\overline{P}_1^{CG}$	4 MW	$\overline{P}_2^{CG}$	6 MW	$\overline{P}_3^{CG}$	4 MW
c_1^{CG}	225 £/MWh	c_2^{CG}	200 £/MWh	c_3^{CG}	250 £/MWh
α_m^{RE}	1 £/MW^{2}h	α_m^{EL}	20000 £/MW^{2}h	α_m^{NEL}	2000 £/MW^{2}h
α_m^{EV}	5000 £/MW^{2}h	β_m^{EL}	10000 £/MWh	β_m^{NEL}	1000 £/MWh

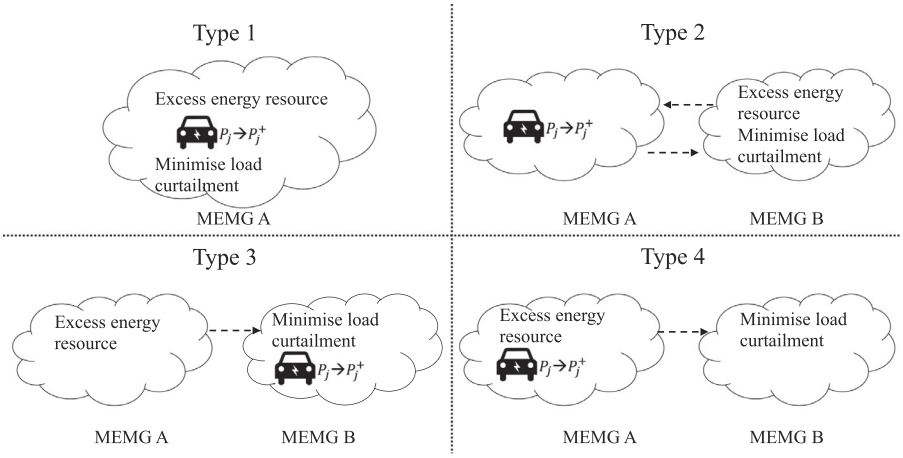

Fig. 8. Spatial and temporal coordination between MEMGs.

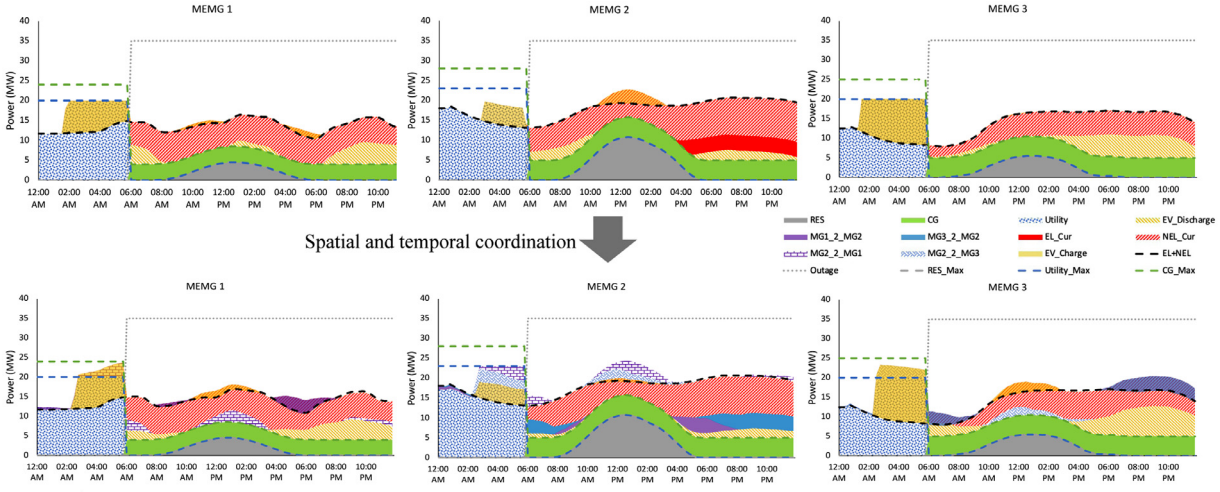

Fig. 9. Energy sources at three MEMGs. Upper row: without MEMG interconnections; Lower row: with MEMG interconnections.

by Type 2, 3, and 4. In Type 2, when the energy resources are redundant, the essential load curtailment is significant, and limited EVs can provide energy shifting operations in MEMG B, resilience enhancement can be achieved through the spatial coordination by using EV flexibility in MEMG A. In Type 3, EVs of MEMG B can absorb the excess energy resources in MEMG A to reduce the local load curtailment. Moreover, EVs in MEMG A can also temporally shift local energy to support the load in MEMG B as shown by Type 4. In addition to mitigating load curtailment, these coordination strategies can also potentially avoid the local network congestion because of the temporal and spatial flexibility of EVs. As a result, the value of EVs is further increased through providing resilience to other MEMGs.

The energy sources in the three MEMGs by using proposed iterative coordination strategy are shown in Fig. 9. Without the interconnection between MEMGs, EVs provide V2G service only to reduce local load curtailment. The essential loads in MEMG 1 and 3 are fully supported by the local electricity resource together with the EV discharging. Although MEMG 2 has the most amount of local controllable generation and the available PV power among these MEMGs, there is a significant essential load curtailment that is represented by the solid red area because of the limited EV flexibility. While the interconnection lines are established, more electricity power in MEMG 2 before the disruptive event is delivered to charge EVs in the other two MEMGs and released back to support the essential load after 4:00 PM. By taking advantage of the spatial and temporal coordination, the essential load curtailment in MEMG 2 has been removed.

Furthermore, in a system with multiple MEMGs, the flexibility of demand response in each MEMG and the interconnection capacity can influence the performance of proposed method on load curtailment mitigation. To evaluate the impact of EV distribution and the interconnection capacity on resilience performance, sensitivity studies have been conducted and the resulting essential load curtailment are compared in Fig. 10. According to the interconnection capacity, the simulations are classified into four groups. In each group, there are three scenarios of total EV number. For each scenario, two simulations with different EV distribution in the MEMGs are considered. Overall, it is obvious that the essential load curtailment decreases with the increasing number of total EVs connected to the MEMGs and the increase of interconnection capacity. Specifically, when the interconnection capacity is limited, the amount of essential load curtailment depends on the EV distribution. For example, the essential load of MEMG 3 is fully supported whereas MEMG 2 has a significant curtailment in the scenario of A/A' and interconnection capacity no more than 1 MW. Meanwhile, it is observed that the EV spatial distribution has higher impact on the load curtailment when the EV number is limited. The difference between scenarios A and A' is 1 MWh whereas the gap between scenarios C and C' increases to 3.8 MWh as the EV number decreases. If the interconnection line is reinforced to 4 MW such that there is no power exchange congestion, the load curtailments in these three MEMGs are even which are not affected by the EV distribution, and the total curtailments are significantly reduced, e.g., by 61.5% in scenario A from 38.24 MWh at 0 MW line capacity to 14.73 MWh.

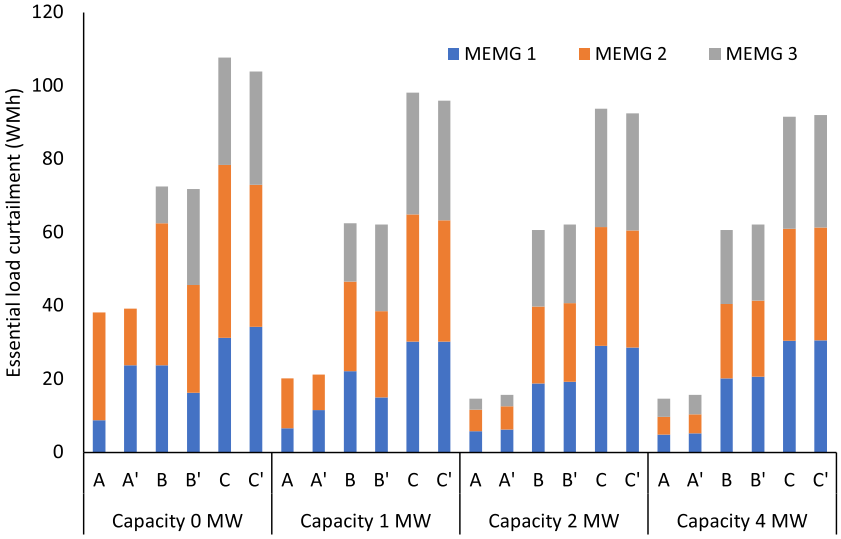

Fig. 10. Essential load curtailment at different EV number and interconnection line capacity scenarios. (A: $N_1 = 2000, N_2 = 1000, N_3 = 3000$, A': $N_1 = 1000, N_2 = 2000, N_3 = 3000$, B: $N_1 = 1000, N_2 = 500, N_3 = 1500$, B': $N_1 = 1500, N_2 = 1000, N_3 = 500$, C: $N_1 = 500, N_2 = 200, N_3 = 300$, C': $N_1 = 300, N_2 = 500, N_3 = 200$)

Moreover, it is also noted that the increase of EV number is more effective to reduce total essential load curtailment at high interconnection capacity, which further implies the superior performance of spatial coordination.

5. Conclusion

In conclusion, this paper proposes a novel distributed optimisation methods for numerous heterogeneous EVs to enhance resilience of an urban energy system. The distributed coordination strategy provides an optimal energy distribution in networked MEMG clusters while performing distribution congestion management and smart load curtailment management. Through effective energy allocations and V2G provision across different MEMGs, the overall curtailment of essential load can be significantly mitigated.

The proposed distributed coordination strategy is firstly applied to a single MEMG system. By using the smart load curtailment management technique, the load curtailment is flattened so that significant fluctuation for the imbalance between demand and supply is avoided. Meanwhile, the total essential load curtailment is reduced by 30% compared to the case where the smart load curtailment management is absent. Regarding the computational performance and optimality, as opposed to the centralised optimisation approach, the distributed algorithm significantly reduces the computational time with less information exchange for a large population of EVs, but the resulting essential load curtailment is slightly higher.

In the second part of simulation, three MEMGs are considered. Results show a considerable benefit of MEMG coordination through interconnection lines to ease the restrictions of uneven distribution of the local resources and the flexibility in different regions. The results show that the essential load curtailment can be further reduced by 61.5% when the interconnection line is reinforced such that there is no power exchange congestion. Furthermore, EVs in different MEMG clusters can exchange energy taking advantage of spatial and temporal flexibility to reduce the overall load curtailment during the outage, which in the meantime provides an opportunity to prevent from local network congestion.

The outstanding performance in load curtailment alleviation and limited computational time make the distributed coordination strategy a promising tool for the operational planning of urban energy systems. Indeed it could be integrated into a rolling horizon control framework to optimise the operation of multi-energy systems in real time. Such extensions of the method will be the research topics of future work.

Declaration of Competing Interest

The authors declare that they have no known competing financial interests or personal relationships that could have appeared to influence the work reported in this paper.

Data availability

Data will be made available on request.

Acknowledgment

This research is supported by the research project: Technology Transformation to Support Flexible and Resilient Local Energy Systems (Grant EP/T021780/1).

References

[1] Rifai HS. Hurricane impacts on critical infrastructure. After Ike: severe storm prediction, impact, and recovery on the Texas Gulf Coast Texas A&M University Press, College Station 2012:122–37.
[2] Office P. Executive August, Economic benefits of increasing electric grid resilience to weather outages. Climate, Energy, and Environment: Issues, Analyses, and Developments 2014;2:89–118.
[3] Motyka M, Slaughter A, Berg J. Reinventing resilience: defining the model for utility-led renewable microgrids. Deloitte 2017.
[4] Stankovic A. The definition and quantification of resilience. IEEE PES Industry Technical Support Task Force: Piscataway, NJ, USA 2018:1–4.
[5] Wu R, Sansavini G. Integrating reliability and resilience to support the transition from passive distribution grids to islanding microgrids. Applied Energy 2020;272:115254.
[6] Wang Y, Rousis AO, Strbac G. On microgrids and resilience: A comprehensive review on modeling and operational strategies. Renewable and Sustainable Energy Reviews 2020;134:110313.
[7] Mishra S, Anderson K, Miller B, Boyer K, Warren A. Microgrid resilience: A holistic approach for assessing threats, identifying vulnerabilities, and designing corresponding mitigation strategies. Applied Energy 2020;264:114726.
[8] Lasseter RH, Paigi P. Microgrid: A conceptual solution. In: 2004 IEEE 35th annual power electronics specialists conference (IEEE Cat. No. 04CH37551), vol. 6. IEEE; 2004. p. 4285–90.
[9] Schneider KP, Tuffner FK, Elizondo MA, Liu C-C, Xu Y, Ton D. Evaluating the feasibility to use microgrids as a resiliency resource. IEEE Transactions on Smart Grid 2016;8(2):687–96.
[10] Xie S, Hu Z, Wang J, Chen Y. The optimal planning of smart multi-energy systems incorporating transportation, natural gas and active distribution networks. Applied Energy 2020;269:115006.
[11] Shang W-L, Chen Y, Ochieng WY. Resilience analysis of transport networks by combining variable message signs with agent-based day-to-day dynamic learning. IEEE Access 2020;8:104458–68.
[12] Kim J, Dvorkin Y. Enhancing distribution system resilience with mobile energy storage and microgrids. IEEE Transactions on Smart Grid 2018;10(5):4996–5006.

[13] Huang W, Zhang X, Li K, Zhang N, Strbac G, Kang C. Resilience oriented planning of urban multi-energy systems with generalized energy storage sources. IEEE Transactions on Power Systems 2021.
[14] Wang D, Qiu J, Reedman L, Meng K, Lai LL. Two-stage energy management for networked microgrids with high renewable penetration. Applied Energy 2018;226:39–48.
[15] Yao S, Wang P, Zhao T. Transportable energy storage for more resilient distribution systems with multiple microgrids. IEEE Transactions on Smart Grid 2018;10(3):3331–41.
[16] Wang C, Yan M, Pang K, Wen F, Teng F. Cyber-physical interdependent restoration scheduling for active distribution network via ad hoc wireless communication. arXiv preprint arXiv: 221102819 2022.
[17] Liu H, Hu Z, Song Y, Lin J. Decentralized vehicle-to-grid control for primary frequency regulation considering charging demands. IEEE Transactions on Power Systems 2013;28(3):3480–9.
[18] Ma Y, Houghton T, Cruden A, Infield D. Modeling the benefits of vehicle-to-grid technology to a power system. IEEE Transactions on power systems 2012;27(2):1012–20.
[19] Turker H, Bacha S. Optimal minimization of plug-in electric vehicle charging cost with vehicle-to-home and vehicle-to-grid concepts. IEEE Transactions on Vehicular Technology 2018;67(11):10281–92.
[20] Shin H, Baldick R. Plug-in electric vehicle to home (v2h) operation under a grid outage. IEEE Transactions on Smart Grid 2016;8(4):2032–41.
[21] Rahimi K, Davoudi M. Electric vehicles for improving resilience of distribution systems. Sustainable cities and society 2018;36:246–56.
[22] Lei S, Chen C, Zhou H, Hou Y. Routing and scheduling of mobile power sources for distribution system resilience enhancement. IEEE Transactions on Smart Grid 2018;10(5):5650–62.
[23] Tian M-W, Talebizadehsardari P. Energy cost and efficiency analysis of building resilience against power outage by shared parking station for electric vehicles and demand response program. Energy 2021;215:119058.
[24] Shang W-L, Chen Y, Li X, Ochieng WY. Resilience analysis of urban road networks based on adaptive signal controls: day-to-day traffic dynamics with deep reinforcement learning. Complexity 2020;2020.
[25] Shang W-L, Gao Z, Daina N, Zhang H, Long Y, Guo Z, Ochieng WY. Benchmark analysis for robustness of multi-scale urban road networks under global disruptions. IEEE Transactions on Intelligent Transportation Systems 2022.
[26] Zheng Y, Niu S, Shang Y, Shao Z, Jian L. Integrating plug-in electric vehicles into power grids: A comprehensive review on power interaction mode, scheduling methodology and mathematical foundation. Renewable and Sustainable Energy Reviews 2019;112:424–39.
[27] Everett III H. Generalized lagrange multiplier method for solving problems of optimum allocation of resources. Operations research 1963;11(3):399–417.
[28] Boyd S, Parikh N, Chu E, Peleato B, Eckstein J, et al. Distributed optimization and statistical learning via the alternating direction method of multipliers. Foundations and Trends® in Machine learning 2011;3(1):1–122.
[29] Shao C, Wang X, Shahidehpour M, Wang X, Wang B. Partial decomposition for distributed electric vehicle charging control considering electric power grid congestion. IEEE Transactions on Smart Grid 2016;8(1):75–83.
[30] Khaki B, Chu C, Gadh R. Hierarchical distributed framework for ev charging scheduling using exchange problem. Applied energy 2019;241:461–71.
[31] Karfopoulos EL, Hatziargyriou ND. Distributed coordination of electric vehicles providing v2g services. IEEE Transactions on Power Systems 2015;31(1):329–38.
[32] Liu M, Phanivong PK, Shi Y, Callaway DS. Decentralized charging control of electric vehicles in residential distribution networks. IEEE Transactions on Control Systems Technology 2017;27(1):266–81.
[33] Yang Y, Jia Q-S, Deconinck G, Guan X, Qiu Z, Hu Z. Distributed coordination of ev charging with renewable energy in a microgrid of buildings. IEEE Transactions on Smart Grid 2017;9(6):6253–64.
[34] Wang L, Chen B. Distributed control for large-scale plug-in electric vehicle charging with a consensus algorithm. International Journal of Electrical Power & Energy Systems 2019;109:369–83.
[35] Cardona JE, López JC, Rider MJ. Decentralized electric vehicles charging coordination using only local voltage magnitude measurements. Electric Power Systems Research 2018;161:139–51.
[36] Zhang Z, Wan Y, Qin J, Fu W, Kang Y. A deep rl-based algorithm for coordinated charging of electric vehicles. IEEE Transactions on Intelligent Transportation Systems 2022.
[37] Bahrami S, Parniani M. Game theoretic based charging strategy for plug-in hybrid electric vehicles. IEEE Transactions on Smart Grid 2014;5(5):2368–75.
[38] Aghajan-Eshkevari S, Azad S, Nazari-Heris M, Ameli MT, Asadi S. Charging and discharging of electric vehicles in power systems: An updated and detailed review of methods, control structures, objectives, and optimization methodologies. Sustainability 2022;14(4):2137.
[39] Nimalsiri NI, Mediwaththe CP, Ratnam EL, Shaw M, Smith DB, Halgamuge SK. A survey of algorithms for distributed charging control of electric vehicles in smart grid. IEEE Transactions on Intelligent Transportation Systems 2019;21(11):4497–4515.
[40] Jiao F, Deng Y, Li D, Wei B, Yue C, Cheng M, Zhang Y, Zhang J. A self-scheduling strategy of virtual power plant with electric vehicles considering margin indexes. Archives of Electrical Engineering 2020;69(4).
[41] Gan L, Chen X, Yu K, Zheng J, Du W. A probabilistic evaluation method of household evs dispatching potential considering users' multiple travel needs. IEEE Transactions on Industry Applications 2020;56(5):5858–67.